Corrosion Inhibition Potential of Aqueous Extract of *Bauhinia acuminata* Linn Leaves on Carbon Steel in Hydrochloric Acid Medium

S. Arun Prabhu[1,], M. Syed Ali Padusha[2,] and S.S. Syed Abuthahir[2,*,]

[1]PG and Research Department of Chemistry, National College (Autonomous) (Affiliated to Bharathidasan University), Tiruchirappalli-620001, India
[2]PG and Research Department of Chemistry, Jamal Mohamed College (Autonomous) (Affiliated to Bharathidasan University), Tiruchirappalli, India

*Corresponding author: E-mail: syedchemjmc@gmail.com

The corrosion of carbon steel in 1 N HCl was analyzed using an aqueous *Bauhinia acuminata* Linn (BaL) leaf extract. Weight loss method was used to determine the inhibitor efficaciousness and corrosion rate. When dissolved in water, a linneus plant leaf extract exhibit an inhibitory effect which is proportionate to the amount of inhibitors present. It is possible to speed up the corrosion process by increasing the inhibitors' concentration. Studies have shown that the BaL leaves extract has a 97.30% inhibitory efficiency. By increasing the concentration of inhibitor solutions, a surface layer forms on carbon steel, which inhibits the activity of the active site. The potentiodynamic polarization (PDP) and AC impedance studies (EIS) were employed to examine the mechanical properties of corrosion inhibition. The surface homogeneity and irregularity of carbon steel were examined using AFM and SEM under polished, corroded and inhibitor-treated surfaces. The surface irregularity of the carbon steel were analyzed using atomic force microscopy.

Keywords: Acidic solutions, Corrosion, *Bauhinia acuminata* Linn, Carbon steel, Mass loss method.

INTRODUCTION

Since the beginning of the industrial revolution, carbon steel has been extensively used in the production of automobiles and other industrial applications due to its structural and reasonably cost, has good physical properties and is compatible with many cutting, welds and coating methods. These characteristic carbon steel allow it to be utilized to make different kinds of panels and frames. Carbon steel beams are often used as building frame material because, like other structural steel beams, they are very robust. Carbon steel also meets the requirements for wind and earthquake stresses. The acidic media are essential to many industrial processes, including pickling, descaling, industrial cleaning, petrochemicals and oil-well acid for oil recovery. As such, their importance in the study of corrosion in carbon steel cannot be emphasized [1-3]. Crude oil was refined under a wide range of hostile conditions. Equipment corrodes and becomes damaged when metals are exposed to industrial acid, which contaminates the circulating acid. In

order to either halt it or at least decrease its influence, inhibitors or additives must be utilized. Industrial processes employ inhibitors to control metal solubility in basic, neutral or acidic conditions.

Using organic compounds as corrosion inhibitors, such as heteroatoms, aromatic rings containing π-electrons and electron donating groups, is an effective technique to stop corrosion [4]. These inhibitors provide a barrier that prevents corrosion on metal surfaces by chemically or physically adhering to the surface. The majority of inhibitors that the general public is aware of are organic compounds made up of heteroatoms, O, N, S and different bond orientations. Wide-ranging effects of corrosion include those that are more harmful to the trustworthy, safe and effective operation of structures or machinery than the simple mass loss of materials themselves [4-6]. Several studies have examined the potential of organic compounds to reduce corrosion in various environments, including neutral, acidic and alkaline conditions [7,8]. These chemical corrosion inhibitors are not commonly used due to their expensive price

and potential harm to the environment. The pursuit of cost-effective and reliable corrosion inhibitors has commenced.

Traditional or herbal medicines have consistently made use of *Bauhinia acuminata* Linn, which belongs to the family Fabaceae. This plant exhibit antioxidant, cholinesterase inhibitor, analgesic, antirheumatic, antibacterial and anti-inflammatory [9,10]. Phthalic acid esters, gallic acid, palmitic acid and ursolic acid have all been isolated in this plant as reported by Vasudevan *et al.* [11]. Whereas hexamethyl cyclotrisiloxane, 1-methyl 3-nonyl indane, β-caryophyllene, α-humulene, isomethyl-α-ionone, α-farnesene, β-ionone, caryophylleneoxide, 1,6,10-dodecatrien-3-ol, 3-hexen-1-ol, caryophyl, humulene epoxide caryophyllene oxide, humulene epoxide, caryophylla-4(12),8 (13)-dien-5α-ol, α-muurolol, α-cadinol and isoaromadendrene were identified in the leaves of *B. acuminata* through GC-MS analysis [12,13].

Corrosion inhibitors can be derived from plant extracts which are known for their environmental benefits [14,15]. The capability of an aqueous extract of *B. acuminata* Linn leaves to preserve carbon steel submerged in 1 N HCl was assessed. The weight loss method was used to study the effects of *B. acuminata* Linn as an effective corrosion inhibitor on the corrosion rate and its efficacy. To gain understanding of the corrosion inhibition mechanism, the potentiodynamic polarization (PDP) and AC impedance studies (EIS) were carried out. The FTIR spectroscopy was used to analyze the protective coating of carbon steel. The SEM images were used to compare smooth carbon steel to polished, corroded, blank and inhibitor treated carbon steel morphology, whereas AFM technique measured the surface roughness and smoothness of carbon steel.

EXPERIMENTAL

Carbon steel specimens: After attaining a mirror surface through a thorough polishing procedure, the materials were carefully degreased using acetone. The composition of the material includes 2.0% carbon, 0.026% sulphur, 0.06% manganese and the remaining amount is iron.

Preparation of stock solutions: To prepare an aqueous extract (100 mL), 10 g of dried plant leaves were boiled in two-fold distilled water. Filtration was used to eliminate the suspended substances and then the solution was concentrated to 100 mL in order to limit corrosion [16]. The analytical grade hydrochloric acid was diluted with double distilled water to obtain a 1 N HCl solution.

Weight loss method: Three polished carbon steel samples were immersed in 1 N HCl with varied extract concentrations for 3 h at room temperature. The mass of each sample was measured before and after the immersion. The inhibition efficiency (%) was calculated using eqn. 1 [17,18]:

$$IE\ (\%) = \frac{CR_1 - CR_2}{CR_1} \times 100 \quad (1)$$

where CR_1 represents the corrosion rate in absence of inhibitor and CR_2 represents the decay rate when the inhibitor is present.

This formula was used to calculate the corrosion rate in mL per day.

$$\text{Corrosion rate (mdd)} = \frac{53.5 \times W}{a \times t} \quad (2)$$

where W is the weight loss in g, a is the area of specimen in cm^2 and t is the exposure time in hours.

Electrochemical studies: The polarization spectroscopy was applied to determine the extent of decomposition inhibition by immersing carbon steel in various concentration solutions. A CHI work station with an impedance model of 660 A was used to conduct the electrochemical investigations in accordance with the procedure.

Polarization studies: A set of three electrodes known as cell assembly was used to conduct polarization studies (Fig. 1). The orientation electrode was established using a conventional calomel electrode (SCE). This work used a platinum counter electrode as well as carbon steel electrode. The results of the polarization analysis were used to evaluate the corrosion characteristic carbon steel [19,20]. The inhibition efficiency (η%) was calculated from the potentiodynamic polarization curves and the electrochemical impedance plots as shown in eqns. 3 and 4, respectively:

$$\eta\% = \frac{j_{corr,0} - j_{corr}}{j_{corr,0}} \times 100 \quad (3)$$

where $j_{corr,0}$ and j_{corr} are the corrosion current density in absence and presence of inhibitor, respectively obtained from Tafel plots.
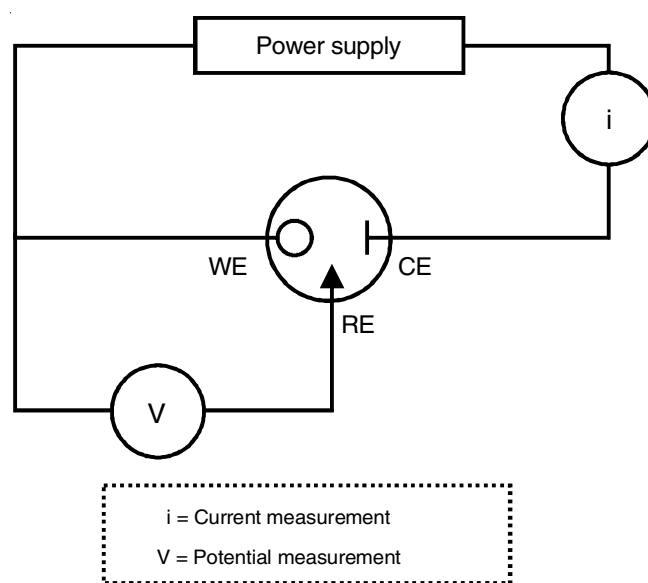
Fig. 1. Three-electrode cell assembly

Furthermore, the charge-resistance obtained from the EIS and fitted employing differential evolution technique with the use of the equivalent electric circuit was used to evaluate the inhibition effect as follows:

$$\eta\% = \frac{R_{ct} - R_{ct,0}}{R_{ct}} \times 100 \quad (4)$$

where $R_{ct,0}$ and R_{ct} are the charge-transfer resistance in absence and presence of inhibitor, respectively. The blank condition was 1 N HCl without inhibitor.

AC impedance spectra: The AC impedance spectra were obtained using the same apparatus and configuration as were utilized for the polarization experiments. The real and imaginary components of the cell resistance were measured at different frequencies using an ohmmeter. The AC impedance spectra were measured using specific parameters: an initial voltage of 0 V, a high frequency range of 1-10^5 Hz, a low frequency of 1 Hz, an amplitude of 0.005 V and a quiet duration of 2 s. The Nyquist plot was analyzed to determine the capacitance of double layer (C_{dl}) and the resistance of charge transfer (R_t) [21].

FTIR analysis: Since several functional groups play an essential role in the inhibitor/surface interactions, the major characteristic groups of *B. acuminata* Linn leaves extract were investigated at room temperature by FT-IR spectroscopy using a Perkin-Elmer spectrophotometer in the range of 4000-400 cm^{-1}. The FTIR spectra were employed to investigate the inhibitory effect of plant leaf extract on the reaction occurring on carbon steel surface. Once the protective layer was removed, the carbon steel was immersed in a solution of 1 N HCl containing leaf extracts as inhibitors at room temperature for 3 h.

Surface analysis: A scanning electron microscopy (SEM) approach was utilized to analyze the surface of carbon steel both before and after being exposed to the corrosive solution, as well as to assess the impact of inhibitor using JEOL Model JSM 6390 SEM instrument.

AFM analysis: The carbon steel sample was submerged in both the inhibitor and blank solutions for 3 h. The surface was thoroughly cleaned using double-distilled water, dried, and subsequently illuminated for analysis [22]. Atomic Force Microscope (AFM) was investigated using Veeco di Innova SPM software version V7.00 to analyze the surface morphology of carbon steel at a scan rate of 0.7 Hz.

RESULTS AND DISCUSSION

Weight loss method: The weight loss measurements in 1 N HCl with and without the aqueous leaf extract of *B. acuminata* Linn, as inhibitor in carbon steel were investigated. At 1000 ppm, *B. acuminata* Linn leaves extract inhibits maximum 97.30% of inhibitory efficacy. Higher concentrations of *B. acuminata* Linn leaves extract increase the corrosion and inhibitory efficiency (IE%) (Table-1). Increasing the inhibitor concentration improves surface coverage and blocks the carbon steel corrosion sites, so enhancing the CR and IE%, which might be explained by the presence of various phytochemicals that limit the dissolving [23,24].

Electrochemical methods: The electrochemical investigations may be implemented to ascertain the corrosion of carbon steel. This technique makes it possible to quickly eval-

TABLE-1
THE CORROSION RATE (CR) AND INHIBITION EFFICIENCY (IE%) OF BaL LEAF EXTRACT ON THE CARBON STEEL CORROSION IN 1 N HCl AT ROOM TEMPERATURE (303 K)

BaL inhibitor leaf extract concentration (ppm)	CR (mdd)	IE (%)
Blank	317.40	–
200	164.10	46.25
400	70.30	76.87
600	55.71	83.95
800	29.74	90.20
1000	12.90	97.30

uate the effectiveness of inhibitors, the resilience of surface coatings and the effectiveness of corrosion inhibitors. In order to analyze carbon steel corrosion in 1 N HCl with and without an inhibitor, we employed these methods to ascertain if the inhibitors worked as cathodic, anodic or mixed inhibitors.

Potentiodynamic polarization (PDP) studies: A protective coating enhances the corrosion current density (I_{corr}) and linear polarization resistance (LPR). Fig. 2 compares the PDP curves of carbon steel in 1 N HCl with and without the inhibitor. Table-2 shows the corrosion potential, current, Tafel slopes, E_{corr}, LPR and I_{corr}. The carbon steel corrosion potential in 1 N HCl was found to be as -464 mV as shown in Fig. 2a, whereas the measured corrosion current was 6.131×10^{-4} A/cm^{-2}. Fig. 2b shows that 1000 ppm inhibitor increases the corrosion potential to the cathodic side (-657 mV/SCE) in corrosive environments. The cathodic side corrosion may affect coated carbon steel. The film forms a compound with Fe^{2+} and inhibitor on carbon steel cathodic sites to modulate the anodic response during dissolution [25-27]. A decrease in I_{corr} and a increase in LPR suggest a better corrosion inhibitor system.
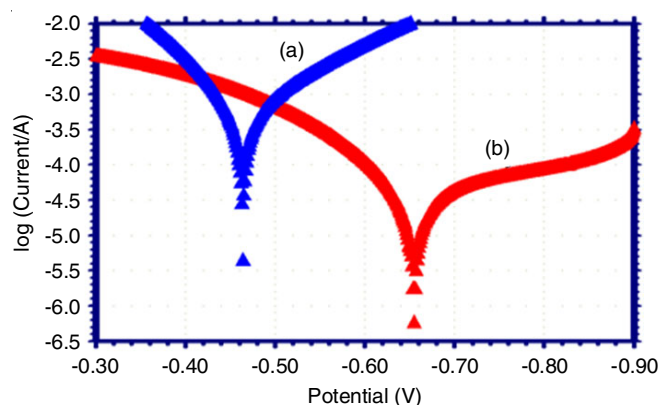
Fig. 2. PDP curves for corrosion (a) carbon steel in 1 N HCl (blank), (b) carbon steel in 1 N HCl with 1000 ppm of BaL leaf extract

AC impedance spectra: AC impedance spectra have been used to accomplish carbon steel surface protection. A protective

TABLE-2
POTENTIODYNAMIC POLARIZATION PARAMETERS FOR THE CORROSION OF CARBON STEEL IN 1 N HCl FOR BaL LEAF EXTRACT SYSTEM

BaL leaf extract concentration (ppm)	E_{corr} (mV/SCE)	Tafel slope		I_{corr} (A/cm^2)	LPR (Ω/cm^2)
		ba (mV/dec)	bc (mV/dec)		
Blank	- 464	10.998	7.175	6.131×10^{-4}	39.0
10	- 657	8.581	2.839	4.889×10^{-5}	770.1

layer covered on the surface of carbon steel results in the increment of all the studied parameters. The AC impedance spectra (Nyquist and Bode plots) in 1 N HCl with inhibitor are shown in Figs. 3 and 4. Table-3 shows the properties of AC impedance, including charge transfer resistance (R_t) and double layer capacitance. The resistance (R_t) and double layer capacitance (C_{dl}) of carbon steel in 1N HCl solution were 12.94 ohm cm² and 1.2727×10^{-7} F cm⁻², respectively. When 1000 ppm of extract was introduced, the R_t increases from 12.94 to 32.32 ohm cm², whereas the C_{dl} value drops significantly from 1.2727×10^{-7} to 5.0959×10^{-8} F cm⁻². The inhibitor system's phase angle has increased to 52º from 43.5º in the blank system [28-31], thereby confirmed that a barrier layer develops on the carbon steel.
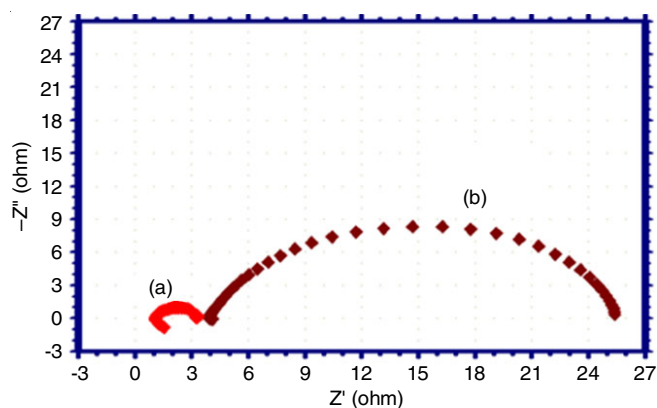
Fig. 3. AC impedance spectra-Nyquist plots (a) carbon steel in 1 N HCl of inhibitor and (b) carbon steel in 1 N HCl with 1000 ppm of BaL leaf extract
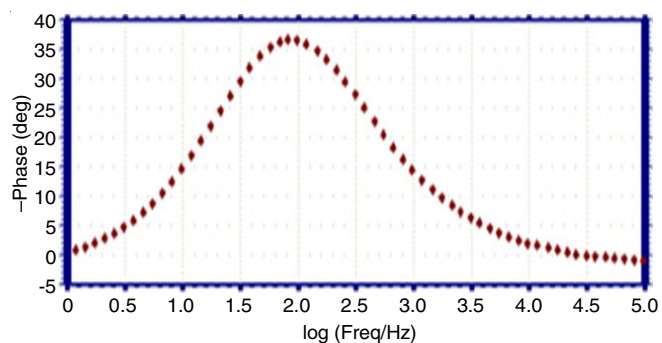
Fig. 4. AC impedance spectra in 1 N HCl with 1000 ppm BaL leaf extract (Bode plot)
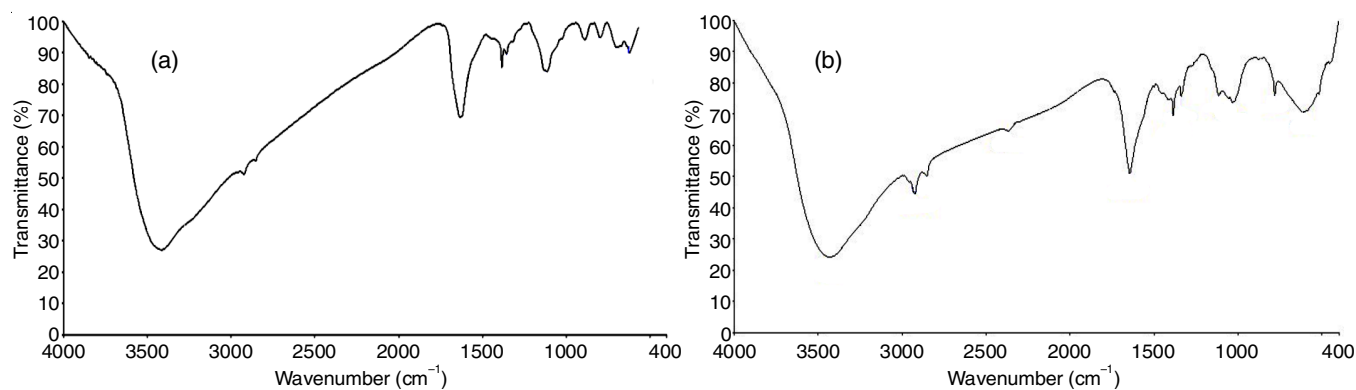
TABLE-3
ELECTROCHEMICAL IMPEDENCE PARAMETERS FROM NYQUIST PLOTS FOR THE CORROSION OF CARBON STEEL FOR BaL LEAF EXTRACT IN 1 N HCl

BaL leaf extract concentration (ppm)	Nyquist plot		Impedance Log (z/ohm)
	R_t (Ω/cm²)	C_{dl} (F/cm²)	
Blank	1.70	2.8×10^{-6}	0.3
1000	8.5	14.0×10^{-6}	0.8

FTIR spectral studies: The protective layer of carbon steel was characterized with FTIR spectral analysis. The FTIR analysis demonstrates the alignment of inhibitor molecules on the carbon steel as well as the presence of absorption bands linked to functional groups. The absorption bands of functional groups present in the related systems are tabulated in Table-4. In the FTIR spectrum before immersion of BaL leaf extract, the peaks at 3417.32, 2925.50, 1613.30, 1363.24, 1116.12 and 693.22 cm⁻¹ are attributed to the -OH, C-H, C=O, C-N, C-C and N-H stretching vibrations, repectively [19,32].

TABLE-4
KEY FTIR SPECTRAL DATA (cm⁻¹) OF BEFORE IMMERSION (a) AND AFTER IMMERSION (b)

IR bands of crude leaves extract of BaL	IR bands of protective layer from carbon steel surface	Frequency assignment to functional groups
3417.32	3433.19	-OH
2925.53	2905.15	C-H stretching
1633.53	1648.03	C-O stretching
1116.20	1113.58	C-C stretching
1366.12	1344.50	C-N
698.22	720.54	N-H
–	604.61	Y-Fe₂O₃

When submerged in 1N HCl solution containing 1000 ppm of BaL aqueous leaf extract, Fig. 5b confirmed the presence of a thin layer that protects carbon steel. A shift in the -OH stretching frequency from 3433.19 to 3417.52 cm⁻¹ suggests that the -OH group is responsible for the adsorption of the molecules [28,33]. Similarly, the other peaks also experienced the some changes in the wavenumbers after the immersion. Most interestingly, a new peak at 604.61 cm⁻¹ appeared, which is attributed to due to the formation of Fe-complex [34], thereby confirmed the formation of protective layer that has been developed on carbon steel.

Fig. 5. FTIR spectrum of BaL leaf extract before immersion (a) and after immersion (b)
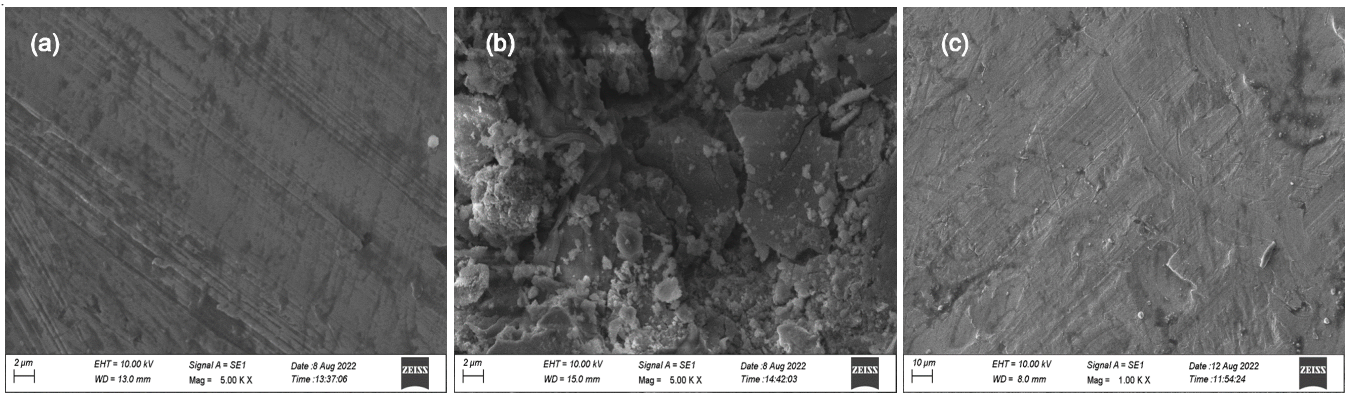
Fig. 6. SEM images of polished carbon steel specimen in control (a), blank (b) and 1 N HCl with 1000 ppm BaL leaf extract (c)

Surface analysis of carbon steel by SEM: The SEM images of carbon steel specimens with and without BaL leaf extract inhibitor system that were immersed in 1N HCl for 3 h are shown in Fig. 6. Fig. 6a shows that polished carbon steel has smooth and clean surface, while a rough surface that has substantial corrosion has been clearly visible in blank sample. The surface of carbon steel with an inhibitor (1000 pm) displayed a smoother and less corroded appearance, attributed to the inhibitor's significant adsorption resulting in the formation of an effective protective film (Fig. 6c). Thus, the inhibitor enhances adsorption efficacy at the carbon steel/solution interface, thereby reducing metallic surface deterioration.

Surface characterization of carbon steel by AFM: There are topographical differences in the formation of protective layers and corrosion on carbon steel depending on the presence or absence of inhibitors. AFM was used to study the effects of corrosion inhibitors on the carbon steel surfaces. Fig. 7 shows

the polished and unpolished carbon steel cross-sectional profiles as well as the 3D AFM morphologies, after 3 h of immersion at room temperature in 1N HCl (with and without BaL leaf extract as inhibitor). The data in Table-5 show that the blank has a high average roughness R_a parameter. The R_a values, which are lower than the blank and higher than the polished carbon steel surface, indicate the presence of a protective layer after immersing carbon steel in 1N HCl with a high concentration of BaL inhibitor aqueous leaf extract [35].

Corrosion causes cracking to appear on the surface of carbon steel (Fig. 7a), while the blank system's polished surface (Fig. 7b) is extremely rough, which demonstrates that in comparison to polished specimens, those in the carbon steel blank method had rougher surfaces. Root mean square roughness (R_q) values for inhibitor systems containing BaL leaf extract are more than polished but less than blank sample. Lower R_q and R_a values are the consequence of the inhibitory qualities of plant leaf extract
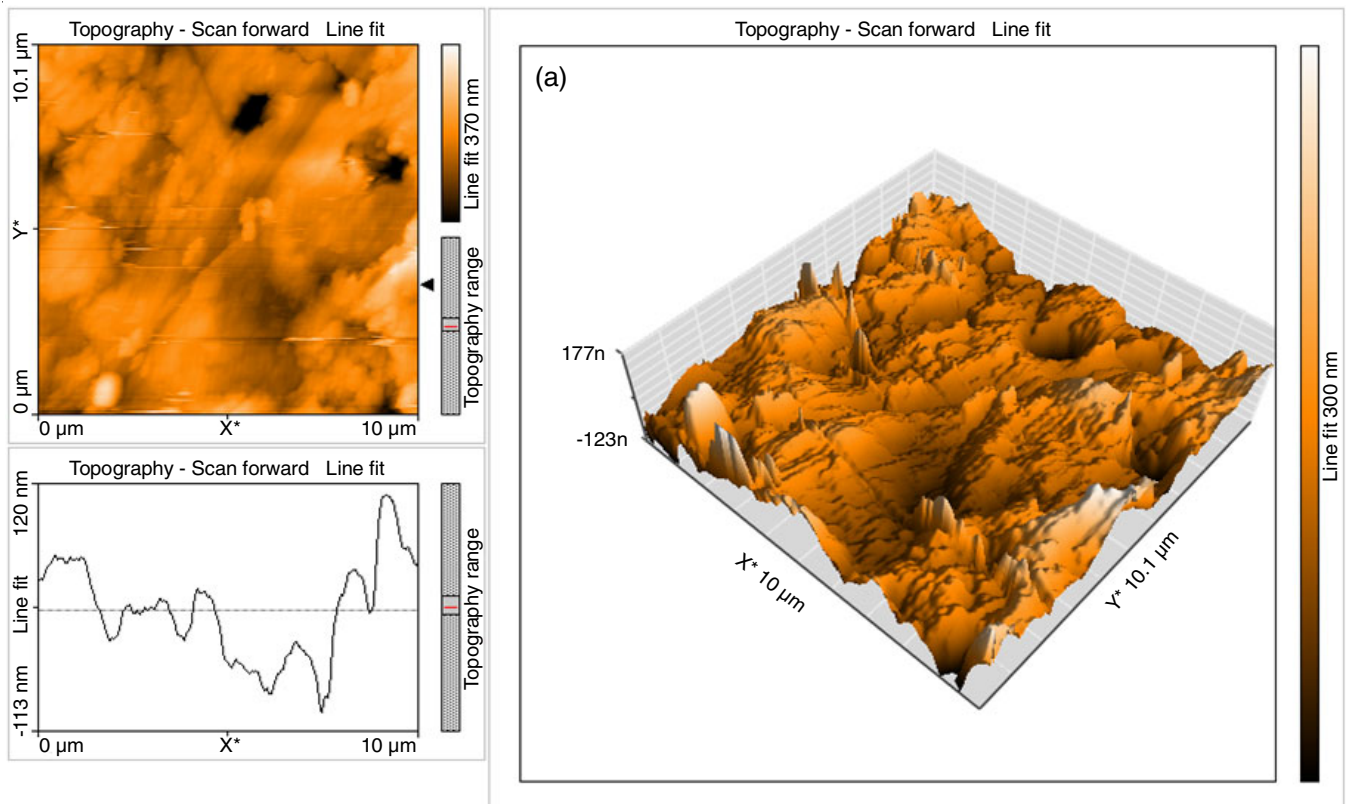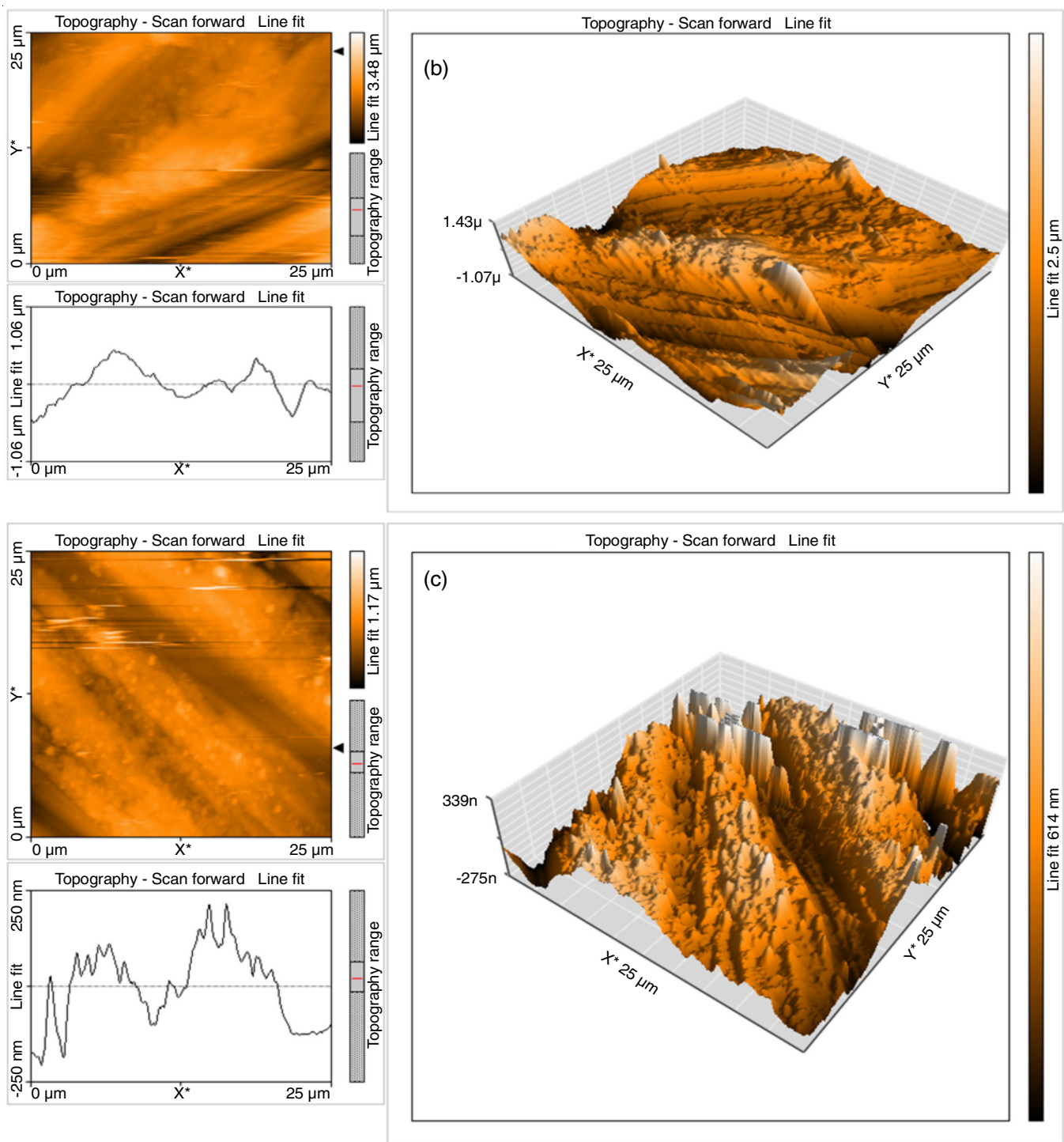
Fig. 7. AFM images of polished carbon steel specimen in control (a), blank (b) and 1 N HCl with 1000 ppm BaL leaf extract (c)

TABLE-5
AFM AND ROUGHNESS DATA FOR CARBON STEEL IMMERSED IN THE
ABSENCE AND PRESENCE OF BaL LEAF EXTRACT AS INHIBITOR

System	Surface roughness (nm)			Line roughness (nm)		
	Average roughness (S_a)	Root mean square roughness (S_q)	Maximum peak to valley (P-V) height	Average roughness (S_a)	Root mean square roughness (S_q)	Maximum peak to valley (P-V) height
Polished carbon steel	31.44	42.38	495.40	33.38	48.774	229.5
Carbon steel + 1 N HCl	273.72	348.79	3334.00	342.25	403.34	1611.94
Carbon steel + 1 N HCl with 1000 ppm of leaves extract of BaL	98.25	120.45	1429.5	86.268	97.969	378.95

molecules being adsorbed on carbon steel. This adsorption method improves the inhibition and successfully postpone the deterioration. The peak-to-valley height is the highest of the five nearby sample heights. When carbon steel is subjected to 1N HCl corrosion, it displays a higher (P-V) height in comparison to polished carbon steel. When compared to polished systems, the height of (P-V) on carbon steel surfaces rises in inhibited systems, but at large inhibitor concentrations, it falls in blank system [36]. In comparison to the polished specimen, the exterior of the carbon steel specimen immersed in 1N HCl without inhibitor seems to be rougher. When carbon steel surfaces are exposed to an acidic solution without inhibitors, they become rough. The carbon steel surface becomes smoother and less rough as a consequence of the inhibitor's protective coating.

The cross-sectional profiles and 3D AFM morphologies showed that the inhibitor had lower values for root mean square roughness (R_q), average roughness (R_a) and peak-to-valley (R_t) compared to the blank studies. The protective coating is composed of nanoscale aqueous leaf extract from the BaL leaf extract inhibitor system in 1N HCl, and the surface is smoothed by layer development, according to these results, which further confirmed with the impedance, polarization, and weight loss method results [37,38].

Conclusion

In present study, an aqueous leaf extract of *Bauhinia acuminata* Linn. was used as green inhibitor on the corrosion of carbon steel corrosion in 1 N HCl medium. The polarization results indicate that the inhibition mechanisms of *B. acuminata* Linn. primarily control the cathodic processes. The inhibition efficiency achieved a value of 97.30% when measured using weight loss method. The progressive thickening of the adsorbed layer leads to an increase in charge transfer resistance (R_t) and decrease in the double layer capacitance (C_{dl}) as well as corrosion current (I_{corr}) values. The FTIR analysis revealed the presence of Fe^{2+}-BAL complex in the protective covering. The SEM images demonstrated the high level of smoothness of polished carbon steel, while the AFM images confirmed the roughness and smoothness of carbon steel surfaces.

CONFLICT OF INTEREST

The authors declare that there is no conflict of interests regarding the publication of this article.

REFERENCES

1. A. Thoume, D.B. Left, A. Elmakssoudi, Z.S. Safi, A. Berisha, R. Kellal, N. Benzbiria and M. Zertoubi, *Mater. Chem. Phys.*, **310**, 128487 (2023); https://doi.org/10.1016/j.matchemphys.2023.128487
2. D. Dwivedi, K. Lepkova and T. Becker, *Proc. R. Soc. A*, **473**, 20160852 (2017); https://doi.org/10.1098/rspa.2016.0852
3. D. Dwivedi, K. Lepková and T. Becker, *RSC Adv.*, **7**, 4580 (2017); https://doi.org/10.1039/C6RA25094G
4. C.I.C. Pinheiro, J.L. Fernandes, L. Domingues, A.J.S. Chambel, I. Graça, N.M.C. Oliveira, H.S. Cerqueira and F.R. Ribeiro, *Ind. Eng. Chem. Res.*, **51**, 1 (2012); https://doi.org/10.1021/ie200743c
5. K. Rose, B.S. Kim, K. Rajagopal, S. Arumugam and K. Devarayan, *J. Mol. Liq.*, **214**, 111 (2016); https://doi.org/10.1016/j.molliq.2015.12.008
6. P. Rao and L. Mulky, *ChemElectroChem*, **10**, e202300152 (2023); https://doi.org/10.1002/celc.202300152
7. A. Khadraoui, A. Khelifa, K. Hachama and R. Mehdaoui, *J. Mol. Liq.*, **214**, 293 (2016); https://doi.org/10.1016/j.molliq.2015.12.064
8. N. Gunavathy and S.C. Murugavel, *J. Environ. Nanotechnol.*, **2**, 45 (2013); https://doi.org/10.13074/jent.2013.12.132049
9. P. Vyas and V.J. Braganza, *Asian J. Pharm. Pharmacol.*, **5**, 834 (2019); https://doi.org/10.31024/ajpp.2019.5.4.26
10. S. Sanjeev and K.R. Raphael, *Int. J. Curr. Pharm. Res.*, **9**, 1 (2017).
11. V. Vasudevan, J. Mathew and S. Baby, *Asian J. Chem.*, **25**, 2329 (2013); https://doi.org/10.14233/ajchem.2013.13282
12. R. Dongray, D. Chanchal and S. Chaudhary, *World J. Pharm. Res.*, **5**, 531 (2016).
13. D. Sebastian and R. Sophy, *Asian J. Pharm. Pharmacol.*, **6**, 164 (2020); https://doi.org/10.31024/ajpp.2020.6.3.2
14. A. El Bribri, M. Tabyaoui, B. Tabyaoui, H. El Attari and F. Bentiss, *Mater. Chem. Phys.*, **141**, 240 (2013); https://doi.org/10.1016/j.matchemphys.2013.05.006
15. P. Mourya, S. Banerjee and M.M. Singh, *Corros. Sci.*, **85**, 352 (2014); https://doi.org/10.1016/j.corsci.2014.04.036
16. L. Li, X. Zhang, J. Lei, J. He, S. Zhang and F. Pan, *Corros. Sci.*, **63**, 82 (2012); https://doi.org/10.1016/j.corsci.2012.05.026
17. M.A. El-Hashemy and A. Sallam, *J. Mater. Res. Technol.*, **9**, 13509 (2020); https://doi.org/10.1016/j.jmrt.2020.09.078
18. V. Sivakumar, K. Velumani and S. Rameshkumar, *Mater. Res.*, **21**, e20170167 (2018); https://doi.org/10.1590/1980-5373-MR-2017-0167
19. S.S.S. Abuthahir, A.J.A. Nasser and S. Rajendran, *Open Mater. Sci. J.*, **8**, 71 (2014); https://doi.org/10.2174/1874088X01408010071
20. S.O. Alharbi, S. Ahmad, T. Gul, I. Ali and A. Bariq, *Sci. Rep.*, **14**, 5098 (2024); https://doi.org/10.1038/s41598-023-47744-y
21. B.-A. Mei, O. Munteshari, J. Lau, B. Dunn and L. Pilon, *J. Phys. Chem. C*, **122**, 194 (2018); https://doi.org/10.1021/acs.jpcc.7b10582
22. R.J. Tuama, M.E. Al-Dokheily and M.N. Khalaf, *Int. J. Corros. Scale Inhib.*, **9**, 427 (2020); https://doi.org/10.17675/2305-6894-2020-9-2-3
23. P.A. Jeeva, G.S. Mali, R. Dinakaran, K. Mohanam and S. Karthikeyan, *Int. J. Corros. Scale Inhib.*, **8**, 1 (2019); https://doi.org/10.17675/2305-6894-2019-8-1-1
24. P. Shanthy, J.A. Thangakani, S. Karthika, S.C. Joycee, S. Rajendran and J. Jeyasundari, *Int. J. Corros. Scale Inhib.*, **10**, 331 (2021); https://doi.org/10.17675/2305-6894-2021-10-1-19
25. P. Mahalakshmi, S. Rajendran, G. Nandhini, S.C. Joycee, N. Vijaya, T. Umasankareswari and N. Renuga Devi, *Int. J. Corros. Scale Inhib.*, **9**, 706 (2020); https://doi.org/10.17675/2305-6894-2020-9-2-20
26. W.M.K.W.M. Ikhmal, M.Y.N. Yasmin, M.F.F. Mari, S.M. Syaizwadi, W.A.W. Rafizah, M.G.M. Sabri and B.M. Zahid, *Int. J. Corros. Scale Inhib.*, **9**, 118 (2020); https://doi.org/10.17675/2305-6894-2020-9-1-7
27. A.G. Baby, S. Rajendran, V. Johnsirani, A. Al-Hashem, N. Karthiga and P. Nivetha, *Int. J. Corros. Scale Inhib.*, **9**, 979 (2020); https://doi.org/10.17675/2305-6894-2020-9-3-12
28. A. Dehghani, G. Bahlakeh, B. Ramezanzadeh and M. Ramezanzadeh, *Constr. Build. Mater.*, **245**, 118464 (2020); https://doi.org/10.1016/j.conbuildmat.2020.118464
29. N. Kicir, G. Tansug, M. Erbil and T. Tüken, *Corros. Sci.*, **105**, 88 (2016); https://doi.org/10.1016/j.corsci.2016.01.006
30. C. Verma, E.E. Ebenso, I. Bahadur and M.A. Quraishi, *J. Mol. Liq.*, **266**, 577 (2018); https://doi.org/10.1016/j.molliq.2018.06.110

31. Y. Zhu, L. Wang, Y. Behnamian, S. Song, R. Wang, Z. Gao, W. Hu and D.H. Xia, *Corros. Sci.*, **170**, 108685 (2020);
https://doi.org/10.1016/j.corsci.2020.108685

32. E. Antony, M. Sathiavelu and S. Arunachalam, *Int. J. Appl. Pharm.*, **9**, 22 (2016);
https://doi.org/10.22159/ijap.2017v9i1.16277

33. S. Karthikeyan, S.S.S. Abuthahir and A.S. Begum, *Int. J. Corros. Scale Inhib.*, **10**, 1531 (2021);
https://doi.org/10.17675/2305-6894-2020-10-4-10

34. S. Karthikeyan and S.S.S. Abuthahir, *Int. J. Biol. Pharm. Allied Sci.*, **10**, 138 (2021).

35. P. Vijayakumar, S. Valarselvan and S.S. Abuthahir, *Port. Electrochem. Acta*, **41**, 1 (2023);
https://doi.org/10.4152/pea.2023410101

36. S. Karthikeyan, S.S. Syed Abuthahir, A.S. Begum and K. Vijaya, *Asian J. Chem.*, **33**, 2219 (2021);
https://doi.org/10.14233/ajchem.2021.23386

37. H.M.K. Sheit, S.M. Kani, M.A. Sathiq, K.S. Mohan and S.S.S. Abuthahir, *High Temp. Corros. Mater.*, **101**, 351 (2024);
https://doi.org/10.1007/s11085-024-10227-0

38. H.M.K. Sheit, S.M. Kani, M.A. Sathiq, S.S.S. Abuthahir, K.S. Mohan, S.B. Mary and K.V. Gunavathy, *Results Surf. Interfaces*, **12**, 100143 (2023);
https://doi.org/10.1016/j.rsurfi.2023.100143